

Twofold Hydrogen Bridges as Observed in Amide-Templated Rotaxanes

Werner Reckien and Sigrid D. Peyerimhoff*

Institut für Physikalische und Theoretische Chemie der Universität Bonn, Wegelerstrasse 12, 53115 Bonn, Germany

Received: February 18, 2003; In Final Form: September 4, 2003

Hydrogen bridges of the type $X-H \cdots A \cdots H-X$, as have been observed in amide-templated rotaxanes, are investigated. The acceptors A are systematically varied by electron withdrawing and electron donating substitutions. A fairly linear relationship between the charge on A or its 1s energies with the bonding strength of the hydrogen bridges is found as long as the X–H moieties retained their character and are placed in a sterically favorable position. The strength of the twofold bridges is about 1.5 times that of a corresponding single hydrogen bond. Changes in the relative position of the two X–H moieties relative to the acceptor A show that steric requirements can dominate charge-transfer properties in hydrogen bonding and point out the importance of proper steric concordance in twofold hydrogen bridges. A search for twofold bridges in biological systems is suggested.

1. Introduction

The synthesis of rotaxanes and even molecular knots has become possible in recent years.¹ Rotaxanes are molecular systems which have a cyclic compound (wheel or ring) threaded onto a linear molecule (axle) with bulky terminal groups (stoppers) to keep the ring from dethreading. The axle is not covalently bound to the ring and has some freedom of motion. For example, the wheel can slide along the axle (possibly in a pirouette motion). Such motion can be used as a mimic of peptide loops that cover protein binding sites.² It has also been observed that the wheel can move between two distinct stations of the axle after photoexcitation by a nanosecond laser pulse.³ This process is reversible and cyclable^{3,4} and has the characteristics of an energy-driven piston. Hence, rotaxanes are also of great importance because they possess key features of nanoscale devices.

A variety of macrocycles and axles have been synthesized and studied.^{1–3,5–9} The character and strength of the axle-ring linkage is of prime interest.² In rotaxanes of the amid type, the axle-shaped moiety is bound to the macrocyclic wheel by a twofold hydrogen bridge. It is assumed that this hydrogen bridge serves as an essential template for the mechanism by which the axle is threaded through the wheel. The two hydrogen-bonding stations in the photoinduced molecular shuttle (the energy driven piston^{3,4}) are of the same type. Details of such twofold hydrogen bridges are not clear, as yet. Experimental studies suggest, however, that template effects based on hydrogen bonding opens a variety of new strategies for the synthesis of supramolecular structures,⁷ among them templates using phenolates,^{10,11} for which we also present theoretical data here.

Because hydrogen bonding plays a pivotal role in biological structures, numerous experimental and theoretical studies have been carried out and various books and review articles can be found in the literature.^{12,13} Generally, the single hydrogen bridge $X-H \cdots A$ is considered, in which a hydrogen atom is attracted to two atoms X and A and acts like a bridge between them.

SCHEME 1: Different Kinds of Hydrogen Bridges



(a) single hydrogen bridge (bond) (c) dihydrogen bond [15]
(b) bifurcated hydrogen bridge (d) twofold hydrogen bridge

The three atoms are preferentially located in a straight line (180°). The X–H group is generally referred to as the proton donor, and A is referred to as the proton acceptor. In some cases, so-called bifurcated hydrogen bonds are also found¹³ where one hydrogen (one donor) builds a bridge with two acceptors A and A' (Scheme 1b). If the acceptors are different, there is often a minor and a major component of the bridge depending on the characteristics of the two acceptors. Such a bifurcated hydrogen bond is also referred to as a “three-center” hydrogen bond in the literature¹⁴ and has been found in calculations of H_2O bonded to HOCHCHOH.

On the other hand, twofold bridges, as observed in the rotaxanes, have not received much attention so far in theory. In this case, two hydrogens share one acceptor (Scheme 1d). This arrangement, in which two (possibly different) donors are linked to one and the same acceptor atom A, is basically different from the bifurcated hydrogen bridge in Scheme 1b in which one donor is H-bonded to two acceptors. In the early literature,¹⁶ various conformers of a water dimer including a “bifurcated” structure similar to that in Scheme 1d have been calculated and theoretically examined, but this structure, as well as a cyclic $(H_2O)_2$ arrangement was found to be energetically less favorable relative to the linear structure (Scheme 1a). In a water trimer, various stationary points on the potential energy surface have recently been determined¹⁷ using symmetry-adapted perturbation theory; this work appeared after submission of our manuscript. In addition to cyclic structures with single hydrogen bridges, a stationary point corresponding to the bifurcated

* To whom correspondence should be addressed.

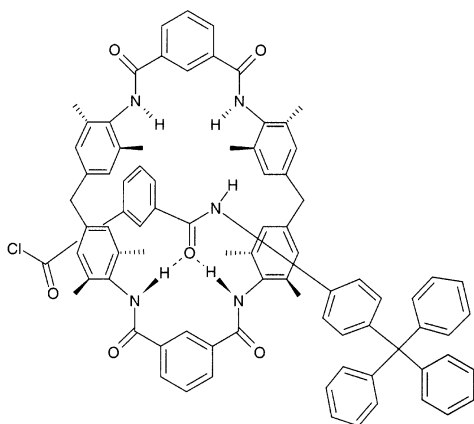


Figure 1. Lock-and-key interaction between the string-like molecule and the eye of a large ring (wheel); in this case through hydrogen bonding between amide groups at the wheel and oxygen in the axle.⁹

arrangement (referred to as *ada*, acceptor–donor–acceptor structure) and one corresponding to the twofold bridge (*dad* structure) were found.

There has recently been some discussion whether such a twofold hydrogen bridge (also referred to as a bifurcated hydrogen bond in these articles) stabilizes guanine tetraplexes^{18–20} or whether the two separate N–H···O bridges (Hoogsteen-bonded structure) are the stabilizing factor. The most recent study²⁰ suggests that hydrogen bonds are weaker in the so-called bifurcated structures than in Hoogsteen guanine tetrads.

Hence, it is the goal of the present work to study twofold hydrogen bridges of the type X–H···A···H–X related to the rotaxanes findings.⁸ Their binding properties, in particular the relation to a single X–H···A bridge, are of prime importance. Furthermore, we want to study to what extent electronic effects modifying the partners X and A influence the properties and what role steric effects play in this regard. The results should not only shed light on the mechanism of dethreading (when the axle slips through the wheel) or the construction of rotaxane

molecular devices but should add to the understanding of hydrogen bridging and could possibly intensify the search for such twofold bridges in biological systems.

2. Systems Investigated

Figure 1 shows a picture of a typical rotaxane precursor⁹ in which the oxygen atom of the C=O group of an amide as part of the axle is the A atom (Scheme 1d) involved in the two hydrogen bridges to the isophthalic amide moiety in the wheel. Because of the size of this system, extensive quantum chemical calculations at a high-level treatment are not feasible. For this reason, a number of smaller model systems are investigated, in which the influence of well-defined modifications on the properties of the twofold hydrogen bridge can be clearly characterized.

In the basic model **1** (Figure 2), the wheel of the rotaxanes is replaced by the representative part involved in the bonding, i.e., by isophthalic amide. The bonding site of the axle is represented by formamide. This model will be successively modified in order to investigate the electronic and steric effects. The charge of the oxygen in the carbonyl group is modified by various substitutions of the formamide using electron withdrawing and electron donating groups (Figure 2). In **2**, the NH₂ group is replaced by N(CH₃)₂, and in **3**, the hydrogens of urea are replaced by CH₃ groups. In **4** and **5**, the formamide is replaced by acetone and formaldehyde, respectively. Compound **6** is related to **4** by replacing the CH₃ groups by CF₃, and **7** is related to **2** by exchanging oxygen by sulfur.

Changes in the charge distribution of the rotaxane wheel are simulated by various substitutions on the phenyl ring of the isophthalic amide (Figure 3). In **8**, an H atom in the meta position is replaced by an OCH₃ group, and in **9** and **10**, a CN group is substituted in meta and in ortho/para position, respectively. In **11**, the oxygen atoms of the isophthalic amide are replaced by sulfur.

Systems in which steric effects may also play a role (Figure 4) are the pyridine derivatives **15** and **16** as well as similar

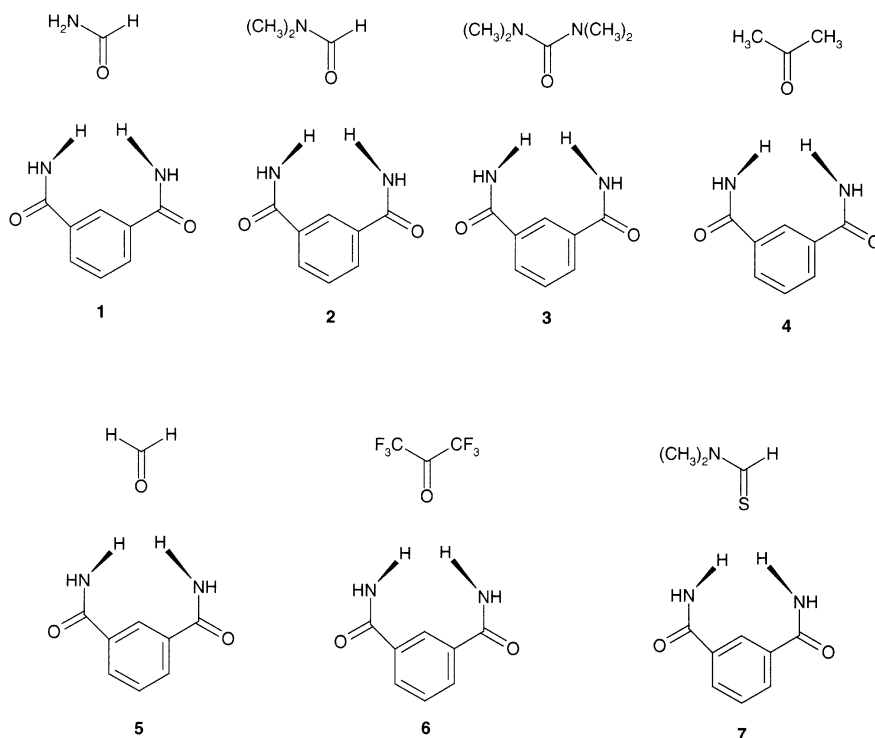


Figure 2. Systems treated: substitutions on the 'axle' moiety.

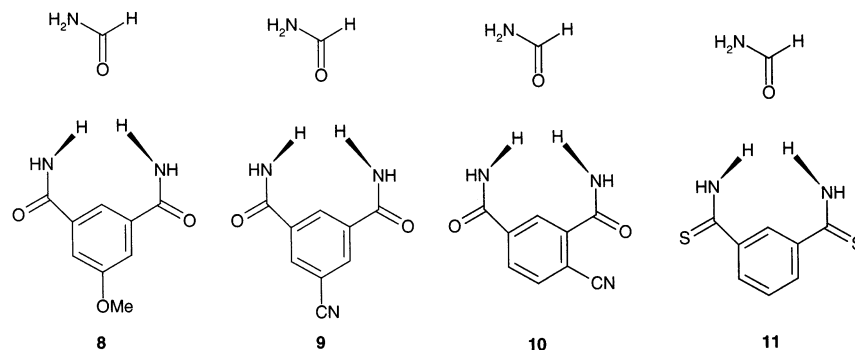


Figure 3. Systems treated: substitutions on the “wheel” moiety.

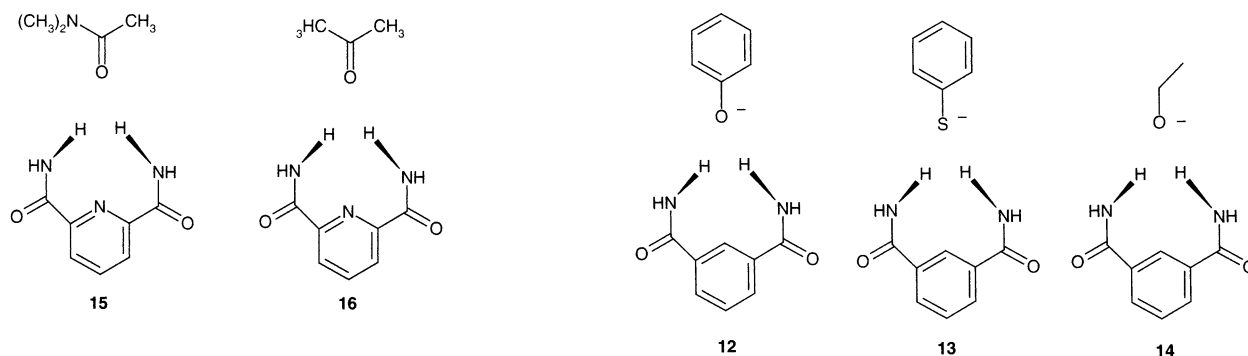


Figure 5. Systems treated: twofold hydrogen bridges with anionic species.

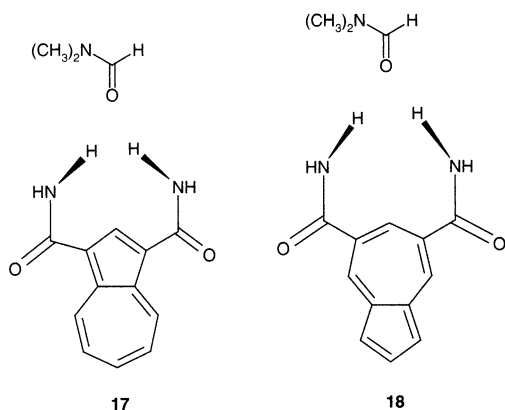


Figure 4. Systems treated: steric effects.

derivatives of the azulene **17** and **18**. In the systems with a pyridine ring, the distance between the two hydrogen atoms of the donor NH_2 groups involved in the bridges is reduced compared to the original isophthalic amide. In the azulene derivatives these NH_2 groups are placed next to the five membered ring in **17** and next to the seven membered ring in **18**. It is apparent that the distance between the two bridging hydrogens is considerably affected by this different geometrical arrangement. It seems to be obvious that the two bridging hydrogens should be located at a favorite geometrical position relative to the acceptor so that an optimal twofold hydrogen bridge can be build. Because azulene possesses a dipole moment (the smaller ring is negatively polarized while the seven membered ring is positively polarized), it will also be interesting to see whether this affects the hydrogen bridge. Finally, large changes are expected if anions are involved in the hydrogen bridging. For this reason, systems **12** (phenolate), **13** (thiolate), and **14** (ethanolate) have been chosen for the hydrogen bridge acceptor (Figure 5).

To compare the twofold hydrogen bridges with single bridges, for all compounds discussed, the corresponding calculations

were also carried out for single hydrogen bonds. In this case, one of the two amide groups of the isophthalic amide was discarded (i.e., replaced by a hydrogen atom).

3. Methods of Calculation

Calculations are first carried out employing the DFT method with the B3LYP²¹ as well as the B3LYP²² functionals in a TZP basis in order to find the optimal geometry for the twofold hydrogen bridges as well as for the systems with the single hydrogen bonds. These were followed by single-point calculations at the respective optimized geometrical arrangement employing a TZVP basis in the RIMP2 treatment,²³ also implemented in the TURBOMOLE 5.4 program.²⁴ To check the reliability of the calculations, several tests using various basis sets (DZ, DZP, TZ, and TZP) and the higher level CCSD treatment as implemented in MOLPRO 2000^{25,26} are undertaken for selected systems. Similarly, the influence of the basis set superposition error (BSSE) is exemplified with the counterpoise correction²⁷ for a few systems. Harmonic vibrational frequencies are taken from the DFT (B3LYP) calculations with a DZP basis, if required.

For the anionic systems, a “negative ion” p function (exponents 0.059 for oxygen, 0.041 for sulfur²⁸) was added to the normal basis sets to account for the more diffuse charge distribution of the negative ion.

Information on the nuclear charges are taken from a population analysis based on the DFT (B3LYP) DZP treatment according to Roby–Davidson–Heinzmann–Ahlrichs^{29–31} as coded in the set of TURBOMOLE programs. Similarly the 1s orbital energy of oxygen in an SCF (DZP basis) calculation is used as indicator for the charge density around the oxygen atom. Because the 1s charge distribution generally does not change from atom to molecule, differences in canonical 1s orbital energies for like atoms directly reflect differences in the valence

TABLE 1: Calculated Bonding Energies (in kcal/mol), Neglecting Zero-Point Energies for the Various Systems Treated^a

	twofold bridge				single bridge		relation	
	RIMP2		RIMP2					
	BHLYP	B3LYP	BHLYP	B3LYP	BHLYP	B3LYP	BHLYP	RIMP2
1	10.5	9.1	9.6	9.4	6.8	6.0	1.54	1.45
2	11.1	9.8	11.8	11.6	7.2	6.4	1.54	1.62
3	12.6	11.2	13.8	13.4	8.0	7.1	1.58	1.57
4	9.3	8.1	9.2	9.1	5.8	5.1	1.60	1.59
5	7.3	6.4	7.1	7.2	4.6	3.9	1.59	1.58
6	3.5	-	5.4	-	2.0	-	1.75	1.74
7	8.3	7.7	-	-	5.9	-	1.41	-
8	10.9	9.5	12.0	11.8	7.0	-	1.56	1.60
9	12.2	10.6	12.2	11.2	8.2	-	1.49	1.47
10	11.5	10.3	11.6	11.7	8.5	-	1.35	1.40
11	11.5	10.2	10.5	10.9	7.2	-	1.60	1.54
12	38.9	-	41.4	-	24.8	-	1.57	-
13	30.9	-	34.8	-	18.8	-	1.64	-
14	53.4	-	54.1	-	35.7	-	1.50	-
15	9.2	8.1	10.7	10.5	-	-	-	-
16	7.2	6.2	8.1	8.0	-	-	-	-
17	8.8	7.5	-	-	6.7	-	1.31	-
18	12.5	10.9	-	-	6.6	-	1.89	-

^a For the twofold hydrogen bridges, the DFT results are listed with the two functionals BHLYP and B3LYP (TZP basis) and the results for the single-point RIMP2 calculations (TZVP basis) at the optimized geometries obtained from the DFT calculations. For the single hydrogen bonds only, the DFT results are given explicitly. The last two columns show the relation between the twofold and the single hydrogen bridge using DFT and RIMP2 results, the latter calculated only for selected examples. Dashes denote that corresponding calculations have not been performed.

charge distribution: the higher the 1s orbital energy the more negative the environment about its corresponding nucleus.³²

4. Results

The calculated bonding energies for the single and for the twofold hydrogen bridge are collected in Table 1. Zero-point energies are neglected; that is, these energies are the difference between total energies of bridged and separated species. Depending on the theoretical treatment, the values show small differences. Generally, the DFT values employing the BHLYP functional are somewhat higher than those using the B3LYP functional. The RIMP2 values are also in basic agreement with those of DFT calculations. Because the results are quite consistent, it seemed unnecessary to perform parallel computations with different methods for all 18 compounds; for this reason RIMP2 and DFT (B3LYP) are done only for a variety of selected systems.

4.1. Reliability of Calculations. The effects of basis sets on the results are studied for system **1** in order to estimate error limits of the calculated data (Table 2). A DZ basis is deficient in the description of polarization and for this reason leads to a geometrical more compact arrangement and a bonding which is too large (without considering the BSSE contribution which is largest in the small AO basis).

The error in the bonding energy is somewhat reduced if a more flexible basis (DZP or TZP) is employed for the amide moiety while the remaining part of the system is still described by the DZ basis. It is also seen that more flexible basis leads to larger differences in the lengths of the twofold hydrogen bridge. The single-point RIMP2 calculation gives a binding energy very close to that of the DFT (BHLYP) calculation. We note that the RI treatment, which uses an auxiliary basis in the MP2 treatment leads in system **1** to a slight lowering of the bonding energy of 0.2–0.4 kcal/mol (Table 2). The energetic and

TABLE 2: Results for 1 Obtained with Different Levels of Treatment^a

	twofold bridge					single bridge		
	R_1	R_2	α_1	α_2	ΔE	R	α	ΔE
DZ	3.10	3.14	177	176	-16.1	2.91	170	-11.0
DZ/DZP	3.13	3.16	177	176	-14.3	3.00	170	-9.4
DZP	3.14	3.21	177	178	-13.1	2.99	169	-9.0
DZ/TZP	3.15	3.19	176	178	-12.2	3.00	170	-7.7
TZP	3.18	3.18	176	175	-10.5	3.02	168	-6.8
AM1	3.13	3.20	162	173	-7.5	3.06	160	-4.8
PM3	3.64	3.68	146	149	-2.9	2.84	166	-2.4
MP2	-	-	-	-	-10.0	-	-	-6.8
RIMP2	-	-	-	-	-9.6	-	-	-6.6

^a All distances R are given in Å, angles α are given in degree, and binding energies ΔE are given in kcal/mol. The nomenclature DZ/DZP indicates that the DZP basis is used for the amide groups while the DZ basis is employed for the isophthalic amide moiety. RIMP2 Calculations are performed with the TZVP basis, MP2 calculations with the TZP basis at the DFT (BHLYP, TZP) geometry. R is the distance between the oxygen and the nitrogen in the isophthalic amide, and α corresponds to the N–H...O angle. R_1 is on the side of the NH₂ group, and R_2 is on the side of the hydrogen.

geometrical trends in going from a DZ to a TZP basis are found in a parallel fashion in the computations for the single hydrogen bonds. In this case, the single bridge is about 0.2 Å shorter than the medium value for the twofold bridge. With these results in mind, we decided to use a TZP basis for all further calculations. This basis has the further advantage that the BSSE, checked for a few cases, is only 0.5 kcal/mol.

The semiempirical AM1 method as implemented in Gaussian 98³³ gives reasonable geometries and underestimates the binding energy in both cases, twofold and single hydrogen bridge, by about 30%. Similar results were already obtained by Buemi et al.³⁴ in their systematic comparison of AM1 and MNDO methods for single X–H–Y hydrogen bonds. They find that hydrogen bonding energies obtained for AM1 computations are better than using MNDO but are still lower than corresponding experimental values and suggest that AM1 results are qualitatively acceptable in this respect. This confirmation is encouraging because it suggests that the AM1 treatment can be employed to give guidelines for twofold hydrogen bridges in larger systems, such as in Figure 1, for which computations as performed in the present work are not feasible any more. The semiempirical PM3³³ procedure is not able to give realistic values for geometry and energy, in particular for the twofold hydrogen bridge. Investigations using the B3LYP functional instead of BHLYP are fully parallel and are therefore not listed here.

Finally, a single-point coupled cluster CCSD calculation has been performed at the BHLYP/TZP geometry employing a DZP basis for a slight modification of system **1**. In this case, the phenyl ring has been omitted in the calculation, but all of the other atoms are kept at their original position in **1** (the dangling carbon bonds are saturated with hydrogens). A parallel DFT (BHLYP) calculation is also performed for this geometrical arrangement, employing the identical DZP basis, and finds that the bonding energy for this structure is higher by 0.7 kcal/mol compared to the full structure **1**. The calculated CCSD bonding energy is 11.9 kcal/mol. If one subtracts 0.7 kcal/mol to account for the omission of the phenyl ring and assumes a similar trend (1.8 kcal/mol) in going from the DZP to the TZP basis (Table 2), the estimated CCSD (TZP) value for **1** would be 9.4 kcal/mol. This value is perfectly in the range of the values obtained in Table 2 from different treatments.

Based on these tests, it is reasonable to assume that the present data are within an error of 2 kcal/mol.

TABLE 3: Charges at the Oxygen Atom According to the RDA^{29–31} Population Analysis (BHLYP/TZP geometry and DZP basis) and Its 1s Orbital Energies (DZP basis, SCF calculation in hartree) for Selected Compounds

charge	ϵ (1s)	charge	ϵ (1s)	charge	ϵ (1s)			
1	-0.438	-20.578	7	-0.369	13	-0.653		
2	-0.466	-20.565	8	-0.463	-20.564	14	-0.809	-20.293
3	-0.542	-20.547	9	-0.444	-20.588	15	-0.478	-20.542
4	-0.346	-20.597	10	-0.442	-20.585	16	-0.336	-20.584
5	-0.252	-20.630	11	-0.442	-20.586	17	-0.490	-20.553
6	-0.209	-20.695	12	-0.747	-20.342	18	-0.474	-20.563

For compound **7** and **13** the charge refers to the sulfur atom.

4.2. Influence of Charges on Bonding. In the system **1**, the H-bond energy of the twofold hydrogen bridge is around 10 kcal/mol. Electron donating substituents, i.e., methyl groups at the nitrogen as in **2** and two such $N(\text{CH}_3)_2$ groups as in **3** increase the bonding energy to 11.8 and 13.8 kcal/mol, respectively (RIMP2 values). On the other hand, if at the carbonyl unit only hydrogen **5** or CH_3 as in acetone **4** is attached instead of the electron donating NH_2 as in **1**, the bonding is reduced to 7 and 9 kcal/mol, respectively. An electron-withdrawing substituent such as CF_3 instead of CH_3 in **6** reduces the bonding energy even further to 4–5 kcal/mol.

These changes can be directly related to the charge at the oxygen which is involved in the twofold hydrogen bridge as seen in Table 3: If the donating part of the model system remains unchanged, the increase (decrease) in the negative charge around the oxygen relative to its value in **1** runs parallel to more (less) bonding. The dependence of the bonding energy on the oxygen 1s orbital energy (Figure 6a) or on the oxygen population is observed to be almost a linear function. Small deviations arise if the twofold bridge is asymmetric because of an asymmetric amide moiety or if the binding energy becomes quite small (with relative large error limits) as in **6**. Replacing oxygen by sulfur (**7** relative to **2**) leads to a less effective binding as expected from the smaller electronegativity of sulfur relative to oxygen.

A very strong H-bond energy is found for the three anionic systems **12–14** with high negative charge around the oxygen (Table 3). The binding is again, as expected, smaller in the sulfur containing compound **13** than in the phenolate **12**. The strongest twofold bridge of all of the compounds treated is seen for ethanolate **14** with a value of 54 kcal/mol.

Substitutions at the wheel have a smaller influence on the strength of the twofold hydrogen bridges than changes at the axle. Introducing an OCH_3 (**8**) or a CN (**9**) group in meta position relative to the amide groups of the isophthalic amide increases the binding strength of the twofold hydrogen bridge by about 1 or 2 kcal/mol relative to **1**. Similarly the CN ortho/para position **10** shows only a small effect compared to its meta-substitution **9**. The calculated charges at the bridging oxygen (Table 3) are essentially the same for **9** and **10**, similar to that in compound **1**, whereas the electron donating OCH_3 substitution **8** matches more the effect seen in **2**. Replacement of the oxygens in the wheel by sulfur **11** seems to have also a very little effect on the charge distribution but rather on the size of the wheel and its cavity. Figure 6b demonstrates that the oxygen 1s orbital energy and the charge obtained for population analysis give essential parallel information for the effective charge at the (oxygen) acceptor site.

4.3. Influence of Steric Effects on Bonding. To analyze steric effects we compared important geometrical parameters (distances between acceptor and the two nitrogens involved ON_1 , ON_2 , the corresponding OHN angles, the NON angle, and the HH and NN separation) obtained from the DFT (BHLYP)

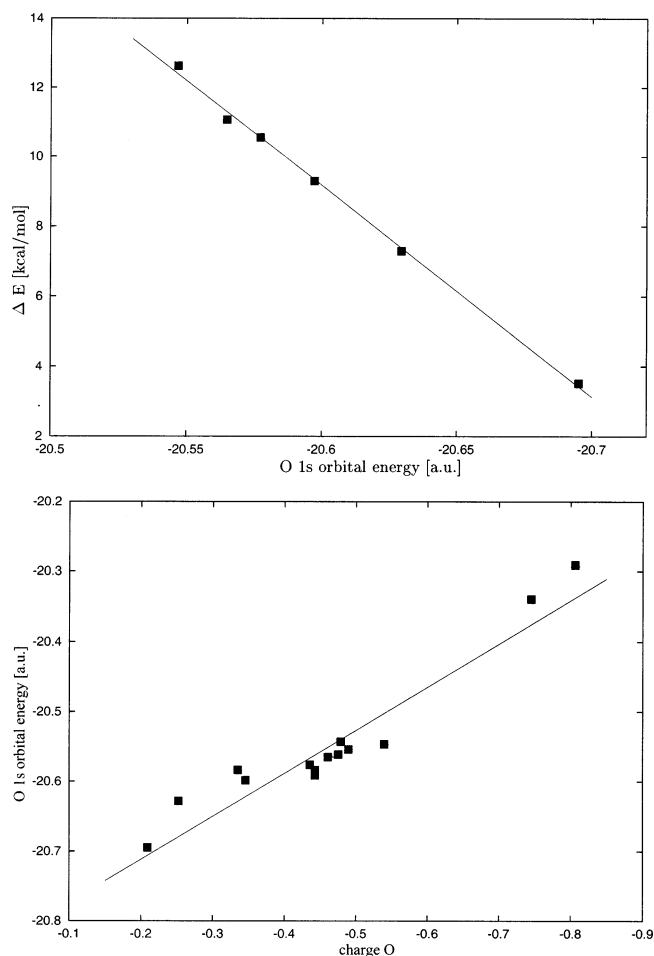


Figure 6. (a) Correlation between H-bond energy and oxygen 1s orbital energy for systems **1–6**. (b) Correlation between oxygen 1s orbital energy and oxygen atomic charges obtained from population analysis for systems.

TABLE 4: Calculated Geometrical Data Obtained from DFT (BHLYP) Calculations for the Twofold Hydrogen Bridge^a

	$R(\text{ON})_1$	$R(\text{ON})_2$	$\angle(\text{OHN})_1$	$\angle(\text{OHN})_2$	$\angle \text{NON}$	$R(\text{HH})$	$R(\text{NN})$
1	3.18	3.18	176	177	104	3.42	5.04
7	3.65	3.64	172	172	90	3.60	5.13
11	3.11	3.12	170	171	103	3.23	4.88
12	2.88	2.88	177	177	115	3.16	4.86
13	3.44	3.44	172	172	95	3.47	5.08
14	2.80	2.80	176	176	118	3.06	4.80

^a Distances are in Å, and angles are in degrees. The subscript denotes the NH_2 side in **1** etc. Note that in **7** and **13**, O must be replaced by S.

calculations. Typical values are presented in Table 4. Considering the compounds **1–5**, it is found that the $\text{O}\cdots\text{H}-\text{N}$ angles are nearly linear ($174\text{--}178^\circ$) as expected for hydrogen bridges. The distances between the carbonyl oxygen and the amide nitrogens at the wheel are between 3.13 Å (**3**) and 3.26 Å (**5**); a direct relation is seen between this distance and the bonding property; that is, the largest bond energy corresponds to the smallest ON separation. The NON angle is around 105° , very close to the equilibrium angle in H_2O . This pattern is distorted in **6**, which shows a larger deviation from the linearity of the $\text{O}\cdots\text{N}-\text{H}$ bond (161°) and the smallest NON angle (99°) compared to those of the first five models. It is conceivable that the steric arrangement of the fluorines and their electronegativity has a prominent effect in this case. The charge density analysis (Table 3) and the largest mean ON bond

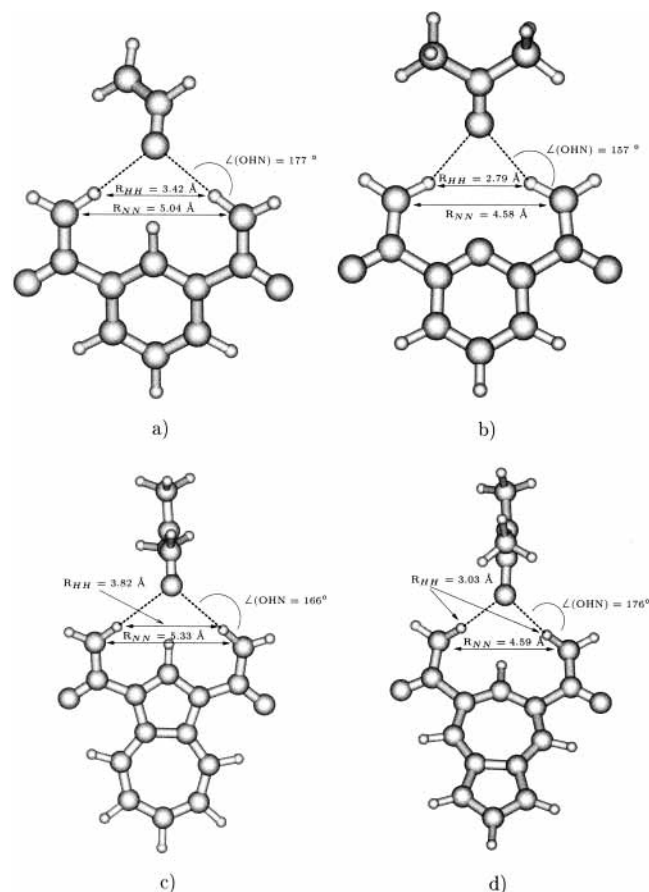


Figure 7. Periment geometrical parameters demonstrating the steric influence on the twofold hydrogen bond. Part a is typical for compounds **1–11**; part b for pyridines **15** and **16**; part c for compound **17**; and part d for **18**.

separation (3.35 Å) are fully in line with the smallest binding energy of **6**.

The heavily bound structures **12** and **14** with the anionic oxygen show the smallest ON separation as expected. As a consequence, the NON angle is increased by 10° while the $\text{O}\cdots\text{H}-\text{N}$ angle remains close to 180° . The $\text{S}\cdots\text{H}-\text{N}$ bond in **13** deviates by 8° from linearity according to the calculations, and the NSN bond angle of 95° is quite close to that in H_2S . In this case, the SN separation is of course larger than the corresponding ON distance because the larger volume of the sulfur atom. It is, however, 0.2 \AA shorter than in the nonionic compound **7** demonstrating its intense bonding properties. If one considers substitution at the wheel, the geometrical parameters for the meta-substitution **8** and **9** are very similar. The model **10** shows different ON bond lengths (3.15 and 3.11 \AA) as a result of the substitution in the ortho/para position.

The pyridine-like compounds **15** and **16** and the two azulene structures **17** and **18** have a different frame than the isophthalic amide. For this reason, the hydrogens are placed in a different position relative to the acceptor oxygen than in all other species treated. The most important sterical consequences are indicated in Figure 7. In **15** and **16**, the NN separation between the two amide groups of the wheel is only about 4.58 \AA . This forces an $\text{O}\cdots\text{H}-\text{N}$ angle of about 157° , i.e., 23° away from the preferred linear arrangement of the bridging atoms. This unfavorable small NN distance is also seen in the small HH separation of 2.79 \AA and the small NON angle of 96° . Although the ON separation is smaller (3.04 \AA) than in the other neutral systems treated so far, the bonding (Table 1) is reduced compared to the other compounds because of the unfavorable steric position of

TABLE 5: Calculated Geometrical Data Obtained from DFT (B3LYP) Calculations for Single Hydrogen Bridges^a

	$R(\text{ON})$	$\Delta R(\text{ON})$	$\angle\text{OHN}$		$R(\text{ON})$	$\Delta R(\text{ON})$	$\angle\text{OHN}$
1	3.02	0.16	168	10	3.00	0.13	173
2	2.99	0.185	173	11	2.98	0.135	166
3	2.96	0.18	173	12	2.74	0.14	177
4	3.06	0.15	171	13	3.35	0.09	168
5	3.11	0.15	170	14	2.53	0.27	178
6	3.25	0.10	169	15			
7	3.50	0.145	162	16			
8	3.00	0.175	169	17	3.02	0.41	167
9	2.99	0.18	173	18	2.97	0.07	172

^a Distances are in Å, and angles are in degrees. The second column shows the difference between twofold and single bridges in the ON distance.

hydrogens in the bridges, even though the negative charge of the oxygen (Table 2) is relative high. The fact that compound **15** shows a smaller bonding energy than **16** with the equivalent steric arrangement of the wheel results, as usual, from the smaller negatively charged oxygen (Table 3).

In the azulene compounds **17** and **18**, the steric requirements place the bridge hydrogens at a distance of 3.82 \AA (**17**) and 3.03 \AA (**18**) from one another, obviously in an unfavorable position compared to those of the models **1–5**. Obviously, **18** is preferred with almost linear $\text{O}\cdots\text{H}-\text{N}$ bridges and a short ON distance (3.04 \AA) relative to **17** ($R_{\text{ON}} = 3.43 \text{ \AA}$). In this case, steric requirements dominate bonding. In **17**, the negative charge at the oxygen is higher and the $1s$ energy lower than in **18** which would prefer bonding in **17** over **18**. The influences of the geometrical data clearly outweigh those of the charge transfer.

4.4. Twofold and Single Hydrogen Bridges. From Table 1, it is seen that the twofold hydrogen bridge is about 1.5 times stronger than the single hydrogen bridge. This finding results from DFT calculations employing the two functionals but also from RIMP2 treatments. As seen for Table 5, the $\text{O}\cdots\text{H}-\text{N}$ angles in the single bridge are very similar to those in the twofold bridges. The ON distances, however, are uniformly shorter in the single bridges by $0.15\text{--}0.20 \text{ \AA}$.

An exception are the systems **15–18**, in which steric effects are the major factor in the strength of the hydrogen bridges. A single hydrogen bond structure involving the inner H atom could not be determined for the pyridine-containing ring. In this case, optimization leads to a structure in which the oxygen builds a linear bridge with the outer H-atom (1.97 \AA) and at the same time the methyl hydrogen of the amide moiety shows some interaction with the oxygen (2.34 \AA) of the “wheel” leading to almost two hydrogen bonds of very different character.

For the azulene structures **17** and **18** the geometrically preferred arrangement in **18** is very similar to the structure in a single hydrogen bridge as seen by the small deviations from the $R(\text{ON})$ and $\angle\text{OHN}$ data (Table 5 and Figure 7). On the other hand the steric strain for the twofold bridge in **17** is released in the single bridge which reduces the $R(\text{ON})$ separation by 0.41 \AA . Indeed, the lower bond energy for **18** relative to **17** in the single hydrogen bridge is in line with the oxygen charges and the $1s$ energies (Table 3). The relatively large relation in **6** might be fortuitous because of the small absolute energies.

It is interesting to see to what extent the isophthalic amide of the wheel is deformed because of the twofold bridge; a single bridge has very little influence on this structure. Table 6 shows important geometrical parameters of the wheel moiety without the bridges. It is seen that the NN separation is decreased in the order of 0.1 \AA in most compounds, with the exceptions of those containing a pyridine ring which exhibit a fairly rigid

TABLE 6: Calculated Geometrical Data (BHLYP) for the Isophthalic Amide Moiety without Hydrogen Bridges

	<i>R</i> (HH)	<i>R</i> (NN)		<i>R</i> (HH)	<i>R</i> (NN)
1–7, 12–14	3.66	5.13	17	4.04	5.43
11	3.53	5.00	18	3.22	4.64
15–16	2.78	4.59			

frame (Table 4 and Figure 7). Similarly, the separation of the two amide hydrogen involved in the hydrogen bonds is decreased in the order of 0.2 Å throughout, again excepting the pyridine structures. In other words, the twofold hydrogen bridge closes slightly the scissors formed by the two NH₂ groups on the wheel.

5. Summary and Conclusion

Based on the twofold hydrogen bridges observed in amide templated rotaxanes we have investigated such bridges in selected model compounds representing the important moieties involved in the bonding between axle and wheel in such rotaxanes. We find that twofold hydrogen bridges of the type N–H···O···H–N have bonding energies up to about 13 kcal/mol in neutral and up to 54 kcal/mol in the anionic systems investigated. Their strength is about 1.5 times the strength of a single hydrogen bridge. In principle, the bonding properties go parallel with the charge at the central oxygen, but in addition, steric effects are essential. In the isophthalic amide moiety, the amide hydrogens are optimally placed so that almost two linear O···H–N bonds with an internuclear HOH angle close to that in H₂O can be formed. If the phenyl ring of the isophthalic amide is replaced by a fairly rigid pyridine ring, the location of the bridge hydrogen atoms relative to the acceptor oxygen is unfavorable and the twofold bridge becomes weaker. The situation is even more enhanced if the phenyl ring is replaced by a azulene moiety as in **17** and **18**. The bonding properties of a single hydrogen bond in these cases are in line with the charge of the acceptor favoring **17** but the steric orientation of the hydrogens in **17** are so unfavorable that the twofold bond is weaker in **17** than in **18**. As a result the general trend that the twofold hydrogen bridge is about 1.5 time the strength of a single bridge is not valid any more.

The present results may be used to explain the different behavior of axles and wheels in the formation or dethreading of rotaxanes and give a clue to the template character of the twofold hydrogen bridge in such systems. They point out basic characteristics of twofold hydrogen bridges and suggest a search for such bridges also in biological systems.

Acknowledgment. This work was supported by the Deutsche Forschungsgemeinschaft in the frame of the SFB 624 (Template). Various helpful discussions with F. Vögtle, C. A. Schalley, and their group members are gratefully acknowledged.

References and Notes

- (1) Sauvage, J. P.; Dietrich-Buchecker, C. *Molecular Catenanes, Rotaxanes and Knots: A Journey Through the World of Molecular Topology*; Wiley-VCH: Weinheim, Germany, 1999.
- (2) Smukste, I.; Smithrud, D. B. *J. Org. Chem.* **2003**, *68*, 2547.
- (3) Brouwer, A. M.; Frochot, C.; Gatti, F. G.; Leigh, D. A.; Mottier, L.; Paolucci, F.; Roffia, S.; Wurple, G. W. H. *Science* **2001**, *291*, 2124.
- (4) Zheng, X.; Sohlberg, K. J. *J. Phys. Chem. A* **2003**, *107*, 1207.
- (5) (a) Glink, P. T.; Oliva, A. I.; Stoddart, J. F.; White, A. J. P.; Williams, D. J. *Angew. Chem.* **2001**, *113*, 1922. (b) Glink, P. T.; Oliva, A. I.; Stoddart, J. F.; White, A. J. P.; Williams, D. J. *Angew. Chem., Int. Ed.* **2001**, *40*, 1870.
- (6) Raymo, F. M.; Houk, K. N.; Stoddart, J. F. *J. Am. Chem. Soc.* **1998**, *120*, 9318.
- (7) Brancato, G.; Coutrot, F.; Leigh, D. A.; Murphy, A.; Wong, J. K. Y.; Zerbetto, F. *PNAS* **2002**, *99*, 4967.
- (8) Reuter, C.; Schmieder, R.; Vögtle, F. *Pure Appl. Chem.* **2000**, *72*, 2233.
- (9) (a) Jäger, R.; Vögtle, F. *Angew. Chem.* **1997**, *109*, 966. (b) Jäger, R.; Vögtle, F. *Angew. Chem., Int. Ed.* **1997**, *36*, 930.
- (10) (a) Hübner, G. M.; Gläser, J.; Seel, C.; Vögtle, F. *Angew. Chem.* **1999**, *111*, 395. (b) Hübner, G. M.; Gläser, J.; Seel, C.; Vögtle, F. *Angew. Chem., Int. Ed.* **1999**, *38*, 383.
- (11) Ghosh, P.; Mermagen, O.; Schalley, C. A. *Chem. Commun.* **2002**, *22*, 2628.
- (12) Desiraju, G. R. *Acc. Chem. Res.* **2002**, *35*, 565.
- (13) (a) Steiner, Th. *Angew. Chem.* **2002**, *114*, 50. (b) Steiner, Th. *Angew. Chem., Int. Ed.* **2002**, *41*, 48.
- (14) Duan, X.; Schreiner, S. *Int. J. Quantum Chem.* **1993**, *Suppl.* *20*, 181.
- (15) Popelier, P. L. A. *J. Phys. Chem. A* **1998**, *102*, 1873.
- (16) (a) Morokuma, K.; Pedersen, L. *J. Chem. Phys.* **1968**, *48*, 3275. (b) Kollman, P. A.; Allen, L. C. *J. Chem. Phys.* **1969**, *51*, 3286. (c) Umeyama, H.; Morokuma, K. *J. Am. Chem. Soc.* **1977**, *99*, 1316.
- (17) Mas, E. M.; Bukowski, R.; Szalewicz, K. *J. Chem. Phys.* **2003**, *118*, 4386.
- (18) Gu, J.; Leszczynski, J.; Bansal, M. *Chem. Phys. Lett.* **1999**, *311*, 209.
- (19) Meyer, M.; Brandl, M.; Sühnel, J. *J. Phys. Chem. A* **2001**, *105*, 8223.
- (20) Louit, G.; Hocquet, A.; Ghomi, M.; Meyer, M.; Sühnel, J. *Phys. Chem. Commun.* **2002**, *5*, 94.
- (21) Becke, A. D. *J. Chem. Phys.* **1993**, *98*, 1372.
- (22) (a) Becke, A. D. *J. Chem. Phys.* **1993**, *98*, 5648. (b) Stephens, P. J.; Devlin, F. J.; Chabalowski, C. F.; Frisch, J. M. *J. Chem. Phys.* **1993**, *98*, 11623.
- (23) (a) Weigend, F.; Häser, M. *Theor. Chem. Acc.* **1997**, *97*, 331. (b) Weigend, F.; Häser, M.; Patzelt, H.; Ahlrichs, R. *Chem. Phys. Lett.* **1998**, *294*, 143.
- (24) Ahlrichs, R.; Bär, M.; Häser, M.; Horn, H.; Kömel, C. *Chem. Phys. Lett.* **1989**, *162*, 165.
- (25) MOLPRO is a package of ab initio programs written by H.-J. Werner and P. J. Knowles, with contributions from R. D. Amos, A. Bernhardsson, P. Celani, D. L. Cooper, M. J. O. Deegan, A. J. Dobbyn, F. Eckert, C. Hampel, G. Hetzer, T. Korona, R. Lindh, A. W. Lloyd, S. J. McNicholas, F. R. Manby, W. Meyer, M. E. Mura, A. Nicklass, P. Palmieri, R. Pitzer, G. Rauhut, M. Schütz, H. Stoll, A. J. Stone, R. Tarroni, and T. Thorsteinsson.
- (26) Hampel, C.; Peterson, K.; Werner, H. J. *Chem. Phys. Lett.* **1992**, *190*, 1.
- (27) Boys, S. F.; Bernardi, F. *Mol. Phys.* **1970**, *19*, 553.
- (28) Dunning, Th. H.; Hay, P. J. *Modern Theoretical Chemistry 3: Methods of Electronic Structure Theory*; Schäfer, H. F., III. Ed.; Plenum Press: New York, 1977.
- (29) Davidson, E. R. *J. Chem. Phys.* **1967**, *46*, 3320.
- (30) Roby, K. R. *Mol. Phys.* **1974**, *27*, 81.
- (31) Heinzmann, R.; Ahlrichs, R. *Theor. Chim. Acta* **1976**, *42*, 33.
- (32) Buenker, R. J.; Peyerimhoff, S. D. *Chem. Phys. Lett.* **1969**, *3*, 37.
- (33) Frisch, M. J.; Trucks, G. W.; Schlegel, H. B.; Scuseria, G. E.; Robb, M. A.; Cheeseman, J. R.; Zakrzewski, V. G.; Montgomery, J. A., Jr.; Stratmann, R. E.; Burant, J. C.; Dapprich, S.; Millam, J. M.; Daniels, A. D.; Kudin, K. N.; Strain, M. C.; Farkas, O.; Tomasi, J.; Barone, V.; Cossi, M.; Cammi, R.; Mennucci, B.; Pomelli, C.; Adamo, C.; Clifford, S.; Ochterski, J.; Petersson, G. A.; Ayala, P. Y.; Cui, Q.; Morokuma, K.; Malick, D. K.; Rabuck, A. D.; Raghavachari, K.; Foresman, J. B.; Cioslowski, J.; Ortiz, J. V.; Stefanov, B. B.; Liu, G.; Liashenko, A.; Piskorz, P.; Komaromi, I.; Gomperts, R.; Martin, R. L.; Fox, D. J.; Keith, T.; Al-Laham, M. A.; Peng, C. Y.; Nanayakkara, A.; Gonzalez, C.; Challacombe, M.; Gill, P. M. W.; Johnson, B. G.; Chen, W.; Wong, M. W.; Andres, J. L.; Head-Gordon, M.; Replogle, E. S.; Pople, J. A. *Gaussian 98*; Gaussian, Inc.: Pittsburgh, PA, 1998.
- (34) Buemi, G.; Zuccarello, F.; Raudino, A. *J. Mol. Structure (THEOCHEM)* **1988**, *164*, 379.